



Production and characterization of standard particles for rL-SNMS

Paul Hanemann¹ · Stefan Bister¹ · Manuel Raiwa¹ · Sandra Reinhard¹ · Darcy van Eerten¹ · Clemens Walther¹

Received: 21 April 2022 / Accepted: 1 October 2022 / Published online: 14 October 2022
© The Author(s) 2022

Abstract

In this work, uranium- and plutonium-bearing particles were produced by fast iron co-precipitation for the purpose of creating homogeneous multi-element standards. A set of single isolated particles showing no inhomogeneities in the element distribution were selected. These particles were used to determine the maximal achievable suppression ratios for uranium in Resonant Laser Secondary Neutral Mass Spectrometry (rL-SNMS) measurements of plutonium. It was shown for the first time directly that suppression-ratios in the order of three magnitudes are achievable with a resonant two-step excitation scheme for non-destructive measurements.

Keywords Resonant laser ionization · Isobaric suppression · U-Pu reference material · Standard particles · Mixed actinide standards

Introduction

Resonant Laser Secondary Neutral Mass Spectrometry (rL-SNMS) combines the isobaric suppression of elemental selective resonant laser ionization with the high sensitivity and spatial resolution of traditional Time of Flight Secondary Ion Mass Spectrometry (ToF-SIMS). In contrast to many other highly potent mass spectrometry methods like Inductively Coupled Plasma Mass Spectrometry (ICP-MS) and Accelerator Mass Spectrometry (AMS), rL-SNMS is a quasi non-destructive method, applicable to many elements. Respective excitation schemes, including nearly all actinides, are reported in the literature [1]. This makes rL-SNMS ideal for the investigation of the isotopic composition of spent nuclear fuel fragments, as evidenced by several publications [2–4].

Despite the high elemental selectivity of resonant laser ionization, one big challenge in the analysis of plutonium isotope ratios in spent nuclear fuel is the isobaric interference of ^{238}Pu and ^{238}U . Analysis by Makarova et al. [5] shows that spent fuel of reactors from the RBMK-1000 class contains up to six orders of magnitude more ^{238}U than ^{238}Pu . Due to this high uranium excess, non-resonantly ionized

^{238}U interferes significantly with ^{238}Pu and the subsequent isotopic ratios for plutonium.

Since these isotope ratios can be used to attribute unknown fuel fragments to their source-term [6–8] precise measurements are of high importance for nuclear forensics applications. It is therefore important to determine the maximum achievable suppression-ratio for uranium in resonant plutonium measurements. Bosco et al. [3] determined the suppression-ratio with a three-step excitation scheme indirectly by comparing the non-resonant background with a resonant measurement and estimating the $^{238}\text{U}/^{238}\text{Pu}$ ratio from the calculated burnup of the sample. The present work aims to determine the suppression-ratio directly by producing and analyzing homogenous U-Pu-reference material.

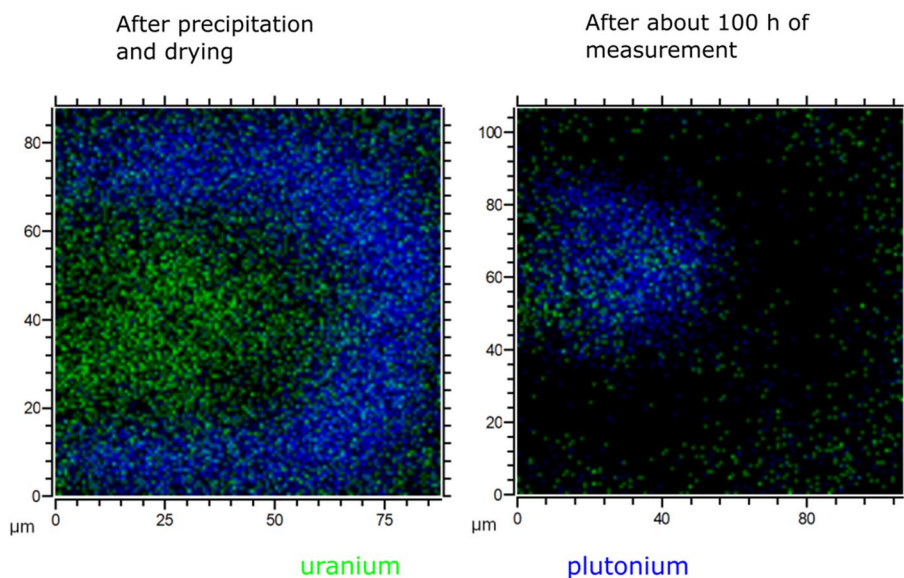
Previous methods to make such material have proved unsuccessful. The simple approach of drying a droplet of mixed U-Pu solution onto an aluminum substrate did not result in a homogenous deposition, but rather showed a clear separation of the elements. Figure 1 shows a spatially resolved rL-SNMS measurement of a dried droplet of dissolved non-irradiated Mixed Oxide Fuel (MOX) in HNO_3 .

The intensity for the resonant measured Pu isotopes is shown in blue, while the sum of the non-resonant ^{238}U , ^{238}UO , $^{238}\text{UO}_2$ signals is shown in green. It is clearly visible, that a separation between both elements took place. It is both spatially separated as seen in the left image after the precipitation and drying of the droplet, but was also revealed to be laterally separated after intense measuring

✉ Paul Hanemann
hanemann@irs.uni-hannover.de

¹ Institute of Radioecology and Radiation Protection,
Herrenhäuser Str. 2, 30419 Hannover, Germany

Fig. 1 Spatially resolved rL-SNMS measurement of dried MOX-droplet before, and after intense measurement



sputtered off layers of the droplet, observed after about 100 h of measurement.

The droplet with a volume of a few nanoliters was produced with a drop-on-demand-printer described by Haas et al. [9]. Figure 1 shows that even at such small volumes, the different solubilities of U and Pu cause separation during the drying process. Right after preparation and drying a coffee-ring type separation [10] is observed. Following the principles set out by Deegan et al. and others observing the droplet drying dynamics of varying compositions [11, 12], it would seem that the less soluble plutonium flows outward ahead of the uranium, leaving the less dense uranium at the center. This is however challenged by the observed changes in droplet composition seen after about 100 h of measurement. After a period of intense measurement, layers of the material have been sputtered off, revealing plutonium at the centre, and uranium deposition around it. As the droplet dries, its volume decreases. Consequently, the concentration of plutonium and uranium in the droplet increases. Plutonium is most likely present in its tetravalent state, uranium as uranyl with oxidation state VI. Pu(IV), due to its lower solubility, precipitates first as an Pu(IV) oxyhydroxide and is afterwards covered by a layer containing the uranium. This explains both the coffee ring structure in the beginning, and that by ablating the surface, the primarily covered plutonium in the central region becomes visible.

Because of this separation, the MOX-droplet is clearly unsuited to the role of spatially homogeneous reference material. This work therefore focuses on another method, that of fast iron-co-precipitation of the two elements. Particles were produced with diameters in the 10 μm range and isolated via the same method used to extract spent fuel particles in environmental samples [13]. Spatially resolved ToF-SIMS measurements were used to identify homogeneous

particles for later analysis. All the rL-SNMS measurements in this work were performed with a two-step excitation scheme for plutonium and the influence of the laser powers on the achievable suppression ratios were investigated. ICP-MS measurements were performed to obtain the element ratios in the particles. The maximal achievable suppression ratios for uranium in resonant plutonium measurements were determined directly on multiple homogeneous particles. To our best knowledge, values presented here for the suppression-ratios are the first values in the literature for non-destructive rL-SNMS measurements with a two-step excitation scheme.

Experimental

For the production of the reference particles, a solution containing ^{242}Pu and a second one, containing depleted uranium solution, containing 99.7% ^{238}U and 0.3% ^{235}U were mixed with an iron-nitrate solution. The solutions were prepared in 4 M HNO_3 for plutonium, in 0.5 M HNO_3 for uranium and 0.1 M HNO_3 for iron. The concentrations and volumes of the solutions were chosen such that the final solution contained 0.32(3) nmol plutonium, 1.0(1) nmol uranium and 90(9) nmol iron. To force a fast precipitation, 2 mL of ammonia were injected into the solution. The precipitate was dried and subsequently washed twice with methanol. After drying it again, the sample was calcinated at 800 $^\circ\text{C}$ for seven hours. The remaining dust, barely visible to the naked eye, was transferred onto carbon tape which serves as a sample holder for the Scanning Electron Microscope (SEM). With a built-in micromanipulator, particles were extracted on tungsten needles for subsequent microanalysis. An SEM image of one of these particles can be found in Fig. 2.

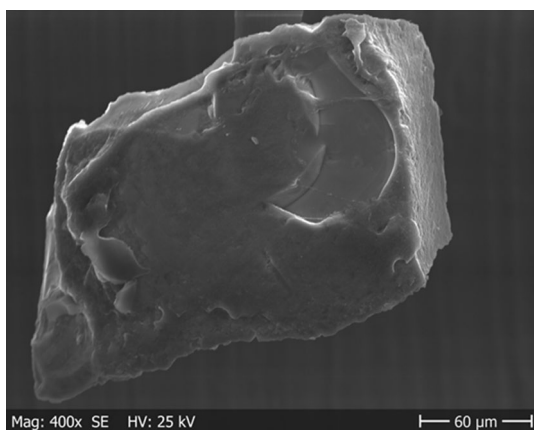


Fig. 2 SEM image of an isolated reference particle

The particle was extracted from the sample surface onto the tungsten needle, visible in the background of the image. The surface of the particle is approximately $200\ \mu\text{m} \times 160\ \mu\text{m}$. It is the biggest particle used in this work.

The rL-SNMS system used in this work is based on a commercially available ToF-SIMS (*ToF.SIMS 5* by *IONTOF GmbH*). It combines a mass resolution of up to $m/\Delta m = 20,000$ with a maximal lateral resolution of 150 nm. To operate in SNMS mode, the sputtered ions are repelled by an electric field, allowing the remaining neutrals to spread for 750 ns, before being selectively ionized by two lasers, and subsequently extracted into the time of flight mass separator. This system is described in more detail in several publications [3, 14–16].

This work uses a two-step laser scheme, described by Raiwa et al. [4]. The lasers used are two intra-cavity frequency doubled titanium-sapphire lasers. Both lasers are equipped with an optical grating in the resonator as the high reflector. Since both gratings are located on an angular actuator, the output wavelength of the system can be adjusted by changing the incident angle of the laser light on the grating. A double-sided anti-reflex blue coated barium borate crystal is used for frequency doubling while also serving as an etalon. Horizontal and vertical adjustments of this crystal by linear actuators are used for both fine tuning and stabilization of the output wavelength and power of the laser-system. The system is automatically operated by control software, which allows stable long time rL-SNMS-measurements [4]. In this work, all rL-SNMS measurements were performed with the same two step excitation scheme for plutonium. The first excitation step (FES) was set to $24,188.7\ \text{cm}^{-1}$, as reported by Blaise et al. [17]. The second excitation step (SES) was set to $24,690.306\ \text{cm}^{-1}$ as developed by Kneip et al. [18]. The laser-powers for these two excitation steps reported in this

paper refer to the power which was measured at the transport-mirror where the two beams merge. The laser power is then focused into the sputtered atom cloud to a diameter of $300\ \mu\text{m}$ [15], ensuring minimal power is lost during the transport. The power values reported here are specific for the used system, and cannot necessarily be directly used on a different experimental setup. The basic reported relationship between laser power and physical effects in the measurements should be applicable for similar setups. Since the beam diameter is smaller than the atom cloud, it is possible to calculate the power density during the ionization. By replicating the power densities for both lasers on a similar setup it should be possible to replicate the results presented here.

For determining the differences in the element ratios of uranium and plutonium in different particles, Energy Dispersive X-ray-spectroscopy (EDX) was performed on single isolated particles. A challenge for these measurements are interferences between the X-ray energies of uranium and plutonium. The M_α energy of plutonium at 3.35 keV is interfered by the M_β energy of uranium at 3.34 keV [19]. This effect makes spatially resolved EDX for investigating the elemental distribution impossible. However, by correcting for the interferences, a comparison of the count-rates from uranium and plutonium is possible. A normalized spectrum of a pure uranium sample can be subtracted from the normalized spectrum of the particle to obtain the plutonium intensity. This method is used throughout this work, as illustrated in Fig. 3.

Both the normalized EDX spectrum of a U-Pu particle and a pure uranium sample are shown in the graph. To obtain the relative plutonium content, the uranium background is subtracted from the U-Pu spectrum. The relative plutonium content is visualized by the orange area, the relative uranium content by the blue area.

Lastly to obtain the absolute element ratios of the particles, ICP-MS measurements were performed on dissolved particles. The used ICP-MS is a commercially available *iCAPQ™* by *Thermo Fischer Scientific*. The particle was dissolved in a mixture of 20 ml sub-boiled HNO_3 and 200 μl of 48% HF. The particles mounted to tungsten needles were separately dissolved in 1.5 ml of that acid at $80\ ^\circ\text{C}$ for 4 h in sealed containers. After that, the needle was rinsed with 0.5 ml of the acid and disposed. The solution with the dissolved particle was evaporated to remove the HF. Finally, 1.5 ml HNO_3 with a concentration of 2% was added. The samples were heated up to $80\ ^\circ\text{C}$ in sealed containers for two hours. After this procedure, the samples were analyzed by ICP-MS. To account for impurities in the used acids or other interferences, an empty tungsten needle was treated identically and used as the reference for the ICP-MS analysis.

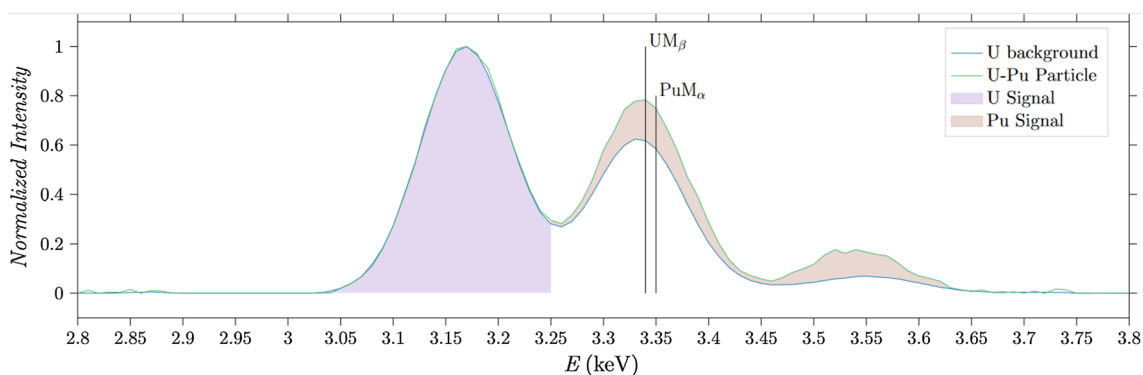


Fig. 3 EDX Spectra

Results and discussion

Spatially resolved ToF-SIMS measurements were performed on isolated reference particles to investigate the homogeneity in the distribution of uranium and plutonium. An overlay of the ^{238}U and the ^{242}Pu signal of one of these measurements is shown in Fig. 4. During the extraction of another particle, it was broken into two pieces. The analysis of the fracture surface showed that no separation of the elements inside of the particle happened. A set of four particles, which didn't show signs of inhomogeneity, were selected for further analysis.

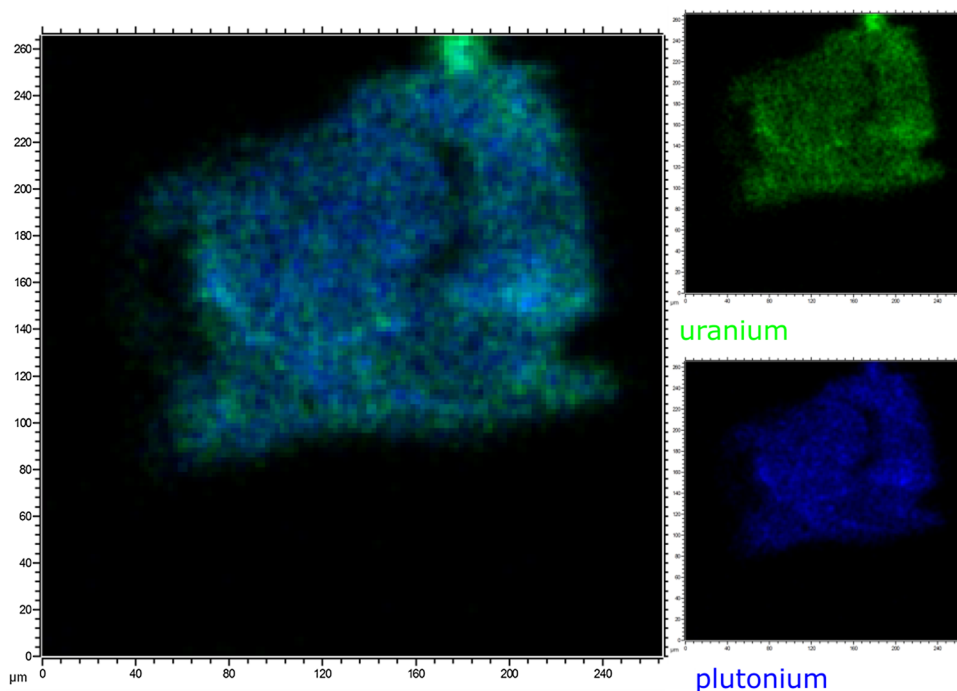
The ^{238}U signal is shown in green, while the ^{242}Pu signal is shown in blue. On the right side both images are shown

separately. Both elements are distributed homogeneously throughout the particle.

Resonant plutonium rL-SNMS-measurements were performed on these particles to investigate the suppression of non-resonant ionized uranium. A scan of the laser powers of the first and second excitation-step was performed on a reference particle to investigate their influence on the maximum achievable suppression ratio. The results of these scans are shown in Fig. 5.

The power-scan of the FES and SES is shown in the graphs. The scan of the FES was performed with a SES-power of 10 mW, the SES-scan with a FES-power of 5 mW. The maximum $^{242}\text{Pu}/^{238}\text{U}$ ratio in the FES-scan was achieved at 5 mW. In the SES-scan, the $^{242}\text{Pu}/^{238}\text{U}$

Fig. 4 Overlay of the ^{242}Pu and ^{238}U signal of a SIMS-measurement



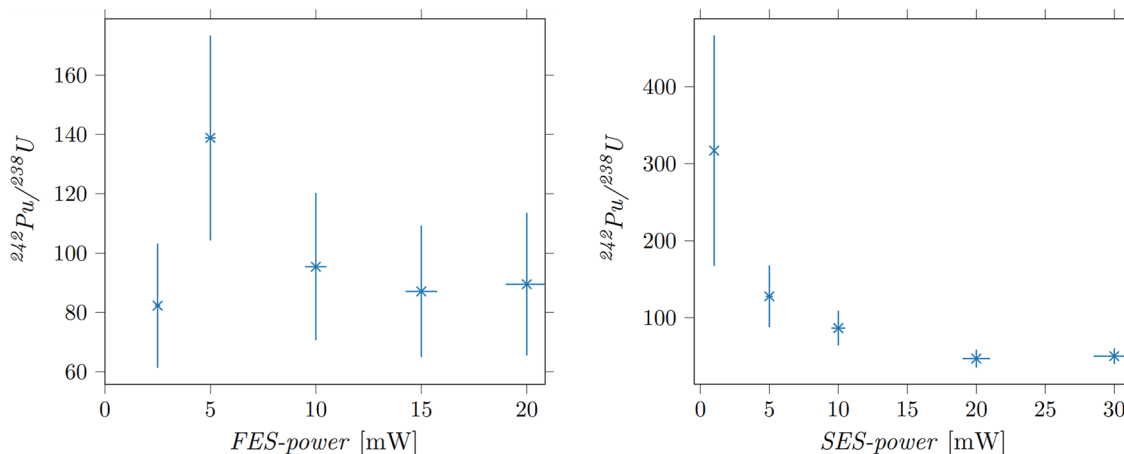


Fig. 5 FES and SES scan

ratio is decreasing with increasing laser power. The laser power was focused to a diameter on 300 μm .

The scan of the FES power showing the highest $^{242}\text{Pu}/^{238}\text{U}$ -ratio is achieved around a power of 5 mW. Below this power, the resonant plutonium signal is increasing with increasing power. After reaching the saturation power, the plutonium signal is no longer amplified by greater powers in a resonant way. Since the non-resonant uranium signal is still increased by higher laser powers, the $^{242}\text{Pu}/^{238}\text{U}$ -ratio decreases for powers greater than 5 mW. With increasing SES power, the $^{242}\text{Pu}/^{238}\text{U}$ -ratio decreases.

Plutonium atoms can only be resonantly ionized by an SES-photon, when they are already excited by a FES-photon. Therefore, a higher SES-power with a fixed FES-power does not lead to a significant increase of the plutonium signal. Since more uranium is non-resonantly ionized by greater SES-power, this leads to the decrease of the $^{242}\text{Pu}/^{238}\text{U}$ -ratio with an increase of the SES-power. Based on these results, all further measurements of the suppression ratio for uranium in resonant plutonium rL-SNMS-measurements in this

work were performed with a FES-power of 5 mW and a SES-power of 1 mW.

On all four particles rL-SNMS-measurements were performed to obtain maximal achievable $^{242}\text{Pu}/^{238}\text{U}$ -ratio for each individual particle. One of the obtained mass spectra is shown in in Fig. 6.

The spectrum shows a resonant plutonium measurement. The plutonium peak at $m/z=242$ is clearly visible. The relative high number of single counts at $m/z=238$ comes from the uranium background.

The results of these rL-SNMS-measurements can be found in Table 1.

The uncertainties of the ICP-MS measurements are calculated analogous to DIN 38 402 [20]. Uncertainties for the rL-SNMS and the EDX are 1σ . Due to the low U count-rate in the rL-SNMS measurements, these and the uncertainties for the maximal achievable suppression-ratio are comparatively high.

EDX was performed on all four particles. The interference-corrected ratio of the intensities from uranium and plutonium is proportional to the element ratio in the particle.

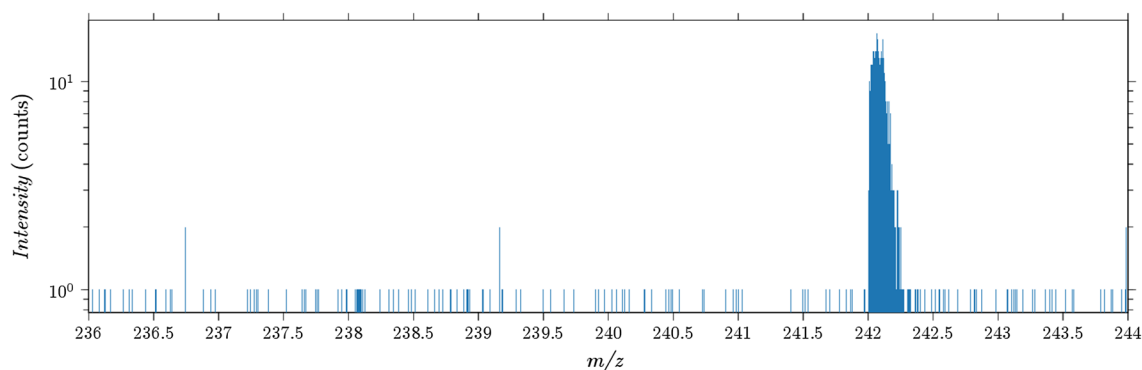


Fig. 6 Spectrum of a rL-SNMS measurement of a reference particle

Table 1 Results of the determination of the maximal achievable suppression-ratio on individual particles

Particle No	Pu/U ratio	Determined by	$^{242}\text{Pu}/^{238}\text{U}$ -ratio in rL-SNMS	Maximal achievable suppression-ratio
1	0.270 ± 0.007	ICP-MS	$(3.2 \pm 0.5) \times 10^2$	$(1.2 \pm 0.2) \times 10^3$
2	0.26 ± 0.02	EDX	$(1.1 \pm 0.3) \times 10^3$	$(4.4 \pm 1.5) \times 10^3$
3	0.29 ± 0.02	ICP-MS	$(1.0 \pm 0.2) \times 10^3$	$(3.6 \pm 0.8) \times 10^3$
4	0.43 ± 0.05	EDX	$(4.1 \pm 0.5) \times 10^2$	$(9.3 \pm 2.3) \times 10^2$
Average suppression-ratio:			2.5×10^3	

After finishing all previous measurements, two particles were dissolved and analyzed with ICP-MS. These measurements were used to establish the element ratio of uranium to plutonium for the particles. It is noticeable that the determined molar ratios correspond well with the molar ratio of the solution that was used to produce the particles. With these values, it is possible to calculate the element ratios of the other particles from the EDX measurements. Together with the $^{242}\text{Pu}/^{238}\text{U}$ -ratio of the rL-SNMS-measurements on the particles and their element ratio, it is possible to determine the suppression of uranium in resonant plutonium rL-SNMS-measurements. The achievable suppression-ratios for uranium against plutonium are in the range of 10^3 . These values are an order of magnitude lower than reported by Bosco et al. [3] with a three-step excitation scheme. This is to be expected, as a two-step excitation scheme has much lower selectivity due to the many non-resonant excitations (of uranium) when using highly energetic blue light. These suppression ratios are high enough that isotope ratios for plutonium, including ^{238}Pu can be measured in burned up fuel by correcting for the non-resonant background, as shown by Raiwa et al. [4].

Conclusions

We showed that fast iron co-precipitation can be used to produce homogeneous uranium–plutonium samples. In contrast to simple methods like using evaporated droplets of characterized U-Pu solutions, it was possible to produce samples without any signs of separation between these two elements. However, the Fe-co-precipitated particles suffer from the dilution effect due to the high iron content. For this reason, comparatively long ToF-SIMS and rL-SNMS measurements have to be performed to obtain sufficient uranium and plutonium signal from the reference particles. The possibility to have much thicker and therefore long-lasting samples and the high sensitivity of rL-SNMS makes up for this minor disadvantage. With the produced reference samples, it was possible to investigate the influence of the FES and SES laser powers on the suppression of uranium in resonant plutonium measurements. It has been determined for the first time that the suppression ratio for a two-step excitation scheme is on

the order of 10^3 , an order of magnitude lower than for a three-step scheme reported in the literature [3].

These values will prove useful for further rL-SNMS measurements on different uranium plutonium mixed samples, such as spent fuel particles from the Chernobyl exclusion zone. The achieved suppression-ratios show that the two-step excitation scheme is sufficient to determine plutonium isotope ratios even in spent nuclear fuel with comparatively low burnup by correcting for the non-resonant ^{238}U background, given sufficient time to measure. Therefore, to the best of our knowledge, we provide the first artificial particles that can be used as reference material for precise measurement of plutonium and uranium isotopic ratios. This isotopic as well as the elemental ratios can be modified to model all types of nuclear material, such as nuclear fuel, residual weapon fallout, or accidental releases. The reference particles can be used for calibration of rL-SNMS systems as well as other types of mass spectrometer used in nuclear forensics. While the presented work focusses on combination of ^{242}Pu and ^{238}U , the inclusion of different plutonium and uranium isotopes will give insight into isotopic ionization efficiencies due to their chemically reproducible precipitation in the iron matrix. In the work described by Raiwa et al. [4] particles containing uranium from an IRMM-2029 isotope reference solution were produced to investigate these isotopic ionization efficiencies.

The iron co-precipitation is a relatively simple method for producing homogeneous multi-element reference particles. It works independent from the chosen elements, meaning it would be possible to investigate suppression-ratios for other relevant isobaric interferences like ^{241}Am and ^{241}Pu .

Acknowledgements The authors would like to thank Jan Heine for the fruitful discussions about data visualization.

Funding Open Access funding enabled and organized by Projekt DEAL.

Open Access This article is licensed under a Creative Commons Attribution 4.0 International License, which permits use, sharing, adaptation, distribution and reproduction in any medium or format, as long as you give appropriate credit to the original author(s) and the source, provide a link to the Creative Commons licence, and indicate if changes were made. The images or other third party material in this article are included in the article's Creative Commons licence, unless indicated otherwise in a credit line to the material. If material is not included in

the article's Creative Commons licence and your intended use is not permitted by statutory regulation or exceeds the permitted use, you will need to obtain permission directly from the copyright holder. To view a copy of this licence, visit <http://creativecommons.org/licenses/by/4.0/>.

References

1. Walther C, Wendt K (2020) Handbook of radioactivity analysis. Academic Press, New York
2. Savina M, Isselhardt B, Trappitsch R (2021) Simultaneous isotopic analysis of U, Pu, and Am in spent nuclear fuel by resonance ionization mass spectrometry. *Anal Chem*. <https://doi.org/10.1021/acs.analchem.1c01360>
3. Bosco H, Hamann L, Kneip N, Raiwa M, Weiss M, Wendt K, Walther C (2021) New horizons in microparticle forensics: actinide imaging and detection of ^{238}Pu and ^{242}mAm in hot particles. *Sci Adv*. <https://doi.org/10.1126/sciadv.abj1175>
4. Raiwa M, Büchner S, Kneip N, Weiß M, Hanemann P, Fraatz P, Heller M, Bosco H, Weber F, Wendt K, Walther C (2022) Actinide imaging in environmental hot particles from Chernobyl by rapid spatially resolved resonant laser secondary neutral mass spectrometry. *Spectrochim Acta B*. <https://doi.org/10.1016/j.sab.2022.106377>
5. Makarova T, Bibichev B, Domkin V (2008) Destructive analysis of the nuclide composition of spent fuel of WWER-440, WWER-1000, and RBMK-1000 reactors. *Radiochemistry*. <https://doi.org/10.1134/S1066362208040152>
6. Wallenius M, Peerani P, Koch L (2000) Origin determination of plutonium material in nuclear forensics. *J Radioanal Nucl Chem*. <https://doi.org/10.1023/A:1006774524272>
7. Lantzou I, Kouvalaki C, Nicolaou G (2015) Plutonium fingerprinting in nuclear forensics of spent nuclear fuel. *Prog Nucl Energ*. <https://doi.org/10.1016/j.pnucene.2015.07.002>
8. Alamelu D, Aggarwal S (2011) Application of chemometry for identification of the source of plutonium. *IJNEST*. <https://doi.org/10.1504/IJNEST.2011.039245>
9. Haas R, Lohse S, Düllmann C, Eberhardt K, Mokry C, Runke J (2017) Development and characterization of a Drop-on-Demand inkjet printing system for nuclear target fabrication. *Nucl Instrum Methods A*. <https://doi.org/10.1016/j.nima.2017.08.027>
10. Deegan D, Bakajin O, Dupont T, Huber G, Nagel S, Witten T (1997) Capillary flow as the cause of ring stains from dried liquid drops. *Nature*. <https://doi.org/10.1038/39827>
11. Lin J, Gentry J (2010) Spray drying drop morphology: experimental study. *Aerosol Sci Tech*. <https://doi.org/10.1080/02786820300888>
12. Davidson Z, Huang Y, Gross A, Martinez A, Still T, Zhou C, Collings P, Kamien R, Yodh A (2017) Deposition and drying dynamics of liquid crystal droplets. *Nat Commun*. <https://doi.org/10.1038/ncomms15642>
13. Extraktion und Analyse uranhaltiger Partikel aus Bodenproben. <https://www.irs.uni-hannover.de/fileadmin/irs/Arbeiten/Bachelor/bachanemann.pdf>
14. Franzmann M, Bosco H, Hamann L, Walther C, Wendt K (2018) Resonant laser-SNMS for spatially resolved and element selective ultra-trace analysis of radionuclides. *J Anal Atom Spectrom*. <https://doi.org/10.1039/C7JA00423K>
15. Franzmann M, Bosco H, Walther C, Wendt K (2017) A new resonant Laser-SNMS system for environmental ultra-trace analysis: installation and optimization. *Int J Mass Spectrom*. <https://doi.org/10.1016/j.ijms.2017.10.003>
16. Mandel M, Holtmann L, Raiwa M, Wunnenberg-Gust A, Riebe B, Walther C (2022) Imaging of I Re and Tc plant uptake on the single-cell scale using SIMS and rL-SNMS. *J Hazard Mater*. <https://doi.org/10.1016/j.jhazmat.2021.127143>
17. Blaise J, Fred M, Gutmacher R (1986) Term analysis of the spectrum of neutral plutonium, Pu I. *J Opt Soc Am B*. <https://doi.org/10.1364/JOSAB.3.000403>
18. Kneip N, Düllmann C, Gadelshin V, Heinke R, Mokry C, Raeder S, Runke J, Studer D, Trautmann N, Weber F, Wendt K (2020) Highly selective two-step laser ionization schemes for the analysis of actinide mixtures. *Hyperfine Interact*. <https://doi.org/10.1007/s10751-020-01712-4>
19. Wiss T, Thiele H, Cremer B, Ray I (2007) Internal conversion in energy dispersive X-ray analysis of actinide-containing materials. *Microsc Microanal*. <https://doi.org/10.1017/S1431927607070365>
20. DIN 38402-13:2021-12 Deutsche Einheitsverfahren zur Wasser-, Abwasser- und Schlammuntersuchung - Allgemeine Angaben (Gruppe A) - Teil 13: Planung und Durchführung der Probenahme von Grundwasser (A 13) (2021). <https://doi.org/10.31030/3274665>

Publisher's Note Springer Nature remains neutral with regard to jurisdictional claims in published maps and institutional affiliations.